Optical Phased Array Antenna Apodization for Lidar in Autonomous Vehicles

José LOZANO [(1)], Humberto JIMENEZ [(1)], Sergio TORRES [(1)], Pau BIOSCA [(1)], Bernat FONTANET [(1)], Jorge PINAZO [(2)], Adolfo LERIN [(2)], Federico DIOS [(1)], Josep R. CASAS [(1)], José A. LÁZARO [(1)]

1. Universitat Politècnica de Catalunya, Jordi Girona 31, E-08034 Barcelona, Spain
2. Capgemini España SL, Dept. I+D, C. del Puerto de Somport, 9, Madrid, Spain

Contact name: José A. Lázaro (jose.antonio.lazaro@upc.edu).

ABSTRACT:

This paper presents the specific design of an Optical Phased Array antenna (OPA) to apodize the emission of a lidar in the context of a project where diverse optoelectronic sensors such as cameras, radars, and commercial lidars are used to provide data in order to fuse them and develop perception for robots as future autonomous vehicles. While mechanical based lidars are already commercially available, this work focuses on designing much more robust and potentially cheaper lidars based on photonic integrated circuits and energy optimization through the apodization of the emission of the OPA.

Key words: Photonic Integrated Circuits, Sensors, Laser, Artificial Intelligence, Autonomous Vehicles, Expressive Robotics, Data Fusion.

1.- Introduction

Expressive robotics is the study and application of how to program robots to react to situations in a manner similar to that of a human. It aims to make interactions between humans and robots straightforward, reassuring, and intuitive. Perception is a crucial aspect of robotics, as it enables machines to interact with the world around them. This paper presents an overview of the main sensors used for AI based AVs and focuses on an apodized OPA as a key element for energy optimized future lidar-on-chip solutions.

2.- Overview on Sensors for Intelligent Perception for AV

Autonomous vehicles have been gaining attention in the past ten years. Level 5 [1] is the idea of a fully autonomous vehicle without a driver, but the first models with level 3 autonomy are only being certified this year 2023 [2]. At this level, the driver must still be in charge in case of unforeseen circumstances or errors in decision-making.

The automotive industry is expected to achieve significant improvements in safety over the coming years, reducing accidents by 15%. The development of the business will increase to 300-400 billion dollars by 2035, showing the importance of the development of intelligent sensors. Vision technologies are driving advancements in perception and interpretation of the environment, with automotive cameras offering higher resolution and image quality. Radar technologies have also made significant strides in the automotive industry. One of the main limitations of radar technology is its low angular resolution compared to alternatives based on Lidar [3]. 4D radar concepts have gained momentum, but safety levels for autonomous vehicles still require higher resolutions. Coherent lidars have also gained prominence, but still have technological challenges to overcome. Initiatives and projects such as INPERCEPT, funded by CDTI, aim to improve these technological aspects to enable a new generation of vehicles while enhancing safety for all users and vulnerable elements in the mobility environment.

2.1.- Radar

MIMO radar is considered key technology for Advanced Driving Assistance Systems

(ADAS), especially in comparison with Lidar, due to the much lower cost, the absence of mechanical parts, its small size, and the ability to work in all weather conditions. MIMO radar with millimetric waves (76-81 GHz) permits good enough both spatial and velocity resolution with a limited size. On the other hand, FMCW has been the most popular modulation scheme up to date, due to the relatively easy and fast signal processing necessary to recover the targets' parameters.

The Digital Code Modulation Radar (DCM) [4] is an alternative to FMCW radar for the automotive industry. It provides a higher resolution in distance, velocity and angular direction measurements, as well as higher resistance to interference. DCM works by modulating the phase of a sinusoidal signal based on a "spread code", which is a sequence of chips (i.e. +1, +1, -1, +1, -1, ...), which represent a sequence of phases (that is, 0, 0, π, 0, π). The signal has a bandwidth proportional to the rate of change of the signal phases, called "chip rate". By comparing the received signal with the transmitted signal (correlation), the radar can determine the distance and speed of reflected objects.

The OFDM RADCOM system combines communication and radar capabilities using OFDM techniques. It uses Fourier transforms (FFT) for signal measurement, and is susceptible to multiuser interference. To mitigate this, the interference cancellation technique involves reconstructing the interference signal and subtracting it from the radar image. The SCA algorithm [5] is used to identify the signal.

2.2.- Cameras

The classic approach in the automotive environment is image analysis from video sensors. However, this approach is limited by being "up to a scale" in the projective domain and lacks depth information for accurate detection and classification. To address this limitation, multi-view analysis techniques such as stereo and structure from motion have been developed. However, deep learning approaches for image analysis have grown and matured rapidly, offering potential for fast and reliable object detection, further improvement in multi-view scenarios, and for combining multi-modal data [6] from different sensors.

2.3.- Lidar

Lidar (Light Detection and Ranging) is a remote sensing technology that uses laser light to measure and map the surrounding environment, Fig. 1, [7]. By analysing the characteristics of the reflected light, lidar sensors can create a high-resolution 3D map of the surrounding environment, which is essential for autonomous cars to make accurate and safe decisions while driving. It is also widely used in other applications, such as robotics, mapping, drone navigation, and atmospheric sensing.

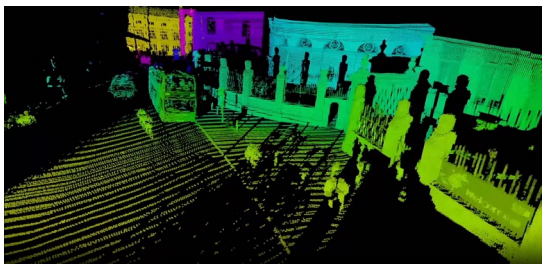

Fig. 1: 3D Point Cloud, reproduced from [8].

2.4.- Sensor Fusion and Artificial Intelligence

Recent research has explored the potential benefits of data fusion across 2D cameras and 3D sensors such as lidar and radar, with the goal of combining strengths of each sensing modality to enable a better understanding of the scene. Data fusion requires precise registration and synchronization, which has been shown to improve accuracy and robustness for object detection. [9].

The automotive industry is exploring the use of cheaper 4D radar sensors to combine 2D and 3D data. This approach involves projecting 3D data onto the camera frame to add a depth component (D) to the initial projected pixels. However, 3D sensors such as lidar and radar are much less dense than megapixel (MPixel) cameras, requiring the use of depth completion (interpolation) models to provide RGB-D images. Lidar-camera fusion has shown promising results in object detection and depth estimation, but lidar sensors can be expensive, prompting the automotive industry to explore the use of cheaper 4D radar sensors.

An approach to sensor fusion [10] involves the use of deep learning to enhance a multi-modal system that combines radar and high-resolution camera sensors. The goal is to train the model to perform inference using cheaper sensors, such as radar, while achieving a solution as close as possible to the learned ground truth (lidar). This approach has shown effectiveness in reconstructing 3D scenes from 2D images and sparse 3D radar data, resulting in a more complete and accurate representation of the environment.

3.- Lidar technology

Numerous market research reports have extensively analysed the market for lidar components, systems, integration platforms, and applications. One key focus has been on the rapidly expanding market segment of automotive lidar. According to a report by BIS Research [11], the automotive lidar market is expected to grow from $353.0 million in 2017 to $8.32 billion by 2028, at a combined annual growth rate of 29.6%, reaching $44 billion by 2050 [12]. A Strategy Analytics report commissioned by Intel predicts a $7 trillion economic impact by 2050 [13]., enabled by the deployment of autonomous vehicles, which will revolutionize the so-called "passenger economy."

3.1.- Lidar requirements

Within the autonomous vehicle industry, lidar systems are expected to meet numerous critical requirements. To provide an overview of these requirements, a list is presented in Fig. 2 detailing the estimated specifications for lidar systems in future autonomous vehicles.

Suggested Automotive LIDAR Performance Specifications

Parameter	Short Range	Long Range
X, Y resolution	~1°	0.1 – 0.15°
Z (depth) resolution	a few cm	
Frame rate	>25 Hz	
Range	20 – 30m	200 – 300m
FOV	>90°	< 90°
Temperature range	AEC-Q100 grade 2 (-40-105C) or better	
Reliability	AEC-Q100	
Laser safety	IEC60825-1 Class 1	
Size	100 – 200 cm^3	
System Cost	$50	$100 - 200

Fig. 2: Lidar requirements for AVs [14].

3.2.- Wavelength

The suitability of different wavelengths for lidar systems in the automotive industry is an important consideration. While the 905nm wavelength is commonly used due to its low cost, high efficiency, and less susceptibility to environmental factors, its range is limited to approximately 100 meters due to safety regulations. The 1550nm wavelength has advantages over the 905nm, including less eye damage and the ability to use higher power with minimized risk [15], resulting in longer range measurements. The use of 1550nm technology is currently limited by its higher cost, but recent advancements in Silicon Photonics are projected to decrease the cost significantly in the near future [16].

In this wavelength, silicon (Si) and silicon nitride (Si_3N_4) are the predominant materials used in optical phased arrays. In [17] the impact of using either material has been analysed, highlighting the superior index contrast of Si, which enables better confinement and smaller device footprints.

3.3.- Types of Lidar

Lidar technology offers several types of systems that are used in various applications, and each has its unique benefits and drawbacks. Among the common types are Rotating Lidar, Micro Electro Mechanical System (MEMS) Lidar, Optical Phased Arrays (OPAs), and Flash Lidar. For AVs, OPAs are a promising option as shown in Fig. 3.

	Rotating	MEMS	OPA	3D Flash
R_{max}	++	+	+	-
FoV	++	+	0	0
Signal-to-Noise Ratio	+	+	++	0
Module Size	-	+	++	+
Robustness	-	+	++	++
Unit Price: 2019	-	0	0	0
Target Price: 2030	0	+	+	+
Product Lifetime	-	+	+	+
Technology Readiness	+	0	-	0

Fig. 3: Lidar technologies comparison [18].

4.- Optical Phased Arrays

Optical phased arrays (OPAs) are solid-state lidars that use an array of small optical elements to steer and control the direction of the coherent laser beam. While OPA technology has made significant progress, developing a low-cost OPA that can be mass-produced for chip-scale optical beam scanners remains a challenge. Achieving the required element

count of 500-1000 [19] for automotive lidars to meet resolution and field-of-view requirements is particularly difficult.

5.- Grating Antenna Apodization

Grating antennas are travelling-wave structures that gradually leak power along its length as Leaky-Wave Antennas (LWAs) from RF technology [20]. They facilitate simple feeding networks, reducing complexity with respect to 2D phased arrays. The radiation pattern is determined by a phase constant β and a leakage factor η, which control the output angle and the rate of the radiation, respectively. There are several types of grating antennas, in our case we will analyse a sidewall grating antenna as shown in Fig. 4.

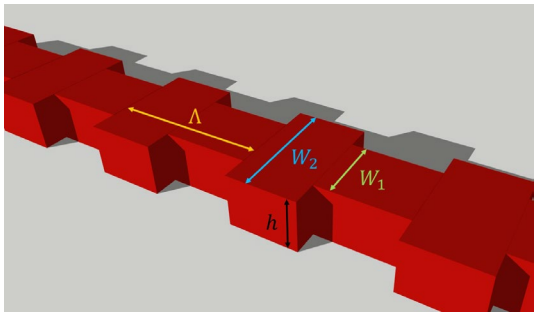

Fig. 4 Sidewall grating antenna

The main waveguide dimensions are $W_1 = 0.5\,\mu m$ and $h = 0.22\,\mu m$. The fundamental mode of this silicon waveguide surrounding by SiO_2 is presented in Fig. 5.

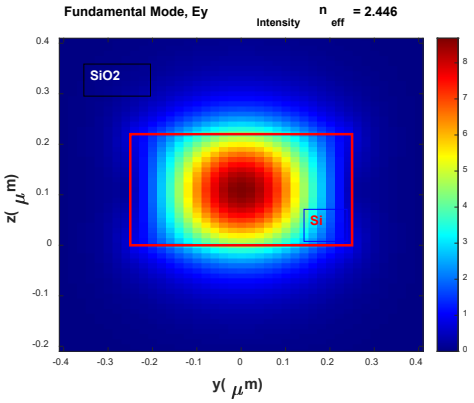

Fig. 5: Fundamental mode at 1.55 μm.

The selection of an appropriate profile is essential for optimizing the performance of grating antennas in various applications. Uniform grating designs exhibit consistent perturbation strength along their entire length, resulting in an exponential decay of light intensity [21]. Additionally, the effective aperture size directly influences the antenna's directivity and operational range. Antenna apodization is a useful technique for optimizing the antenna's emission characteristics. For a 60-element uniform grating antenna, with a height of 0.22μm, $W_1 = 0.5$ μm, $W_2 = 0.8$ μm, $\Lambda = 0.66$ μm and DC = 50%, we can derive the near field profile shown in Fig. 6.

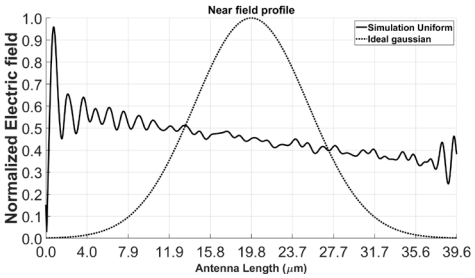

Fig. 6: Near field profile of a uniform grating.

5.1.- Element widths

To generate any propagating profile just above the grating antenna, an apodization is needed. We can create any profile with the help of the model shown in Fig. 7.

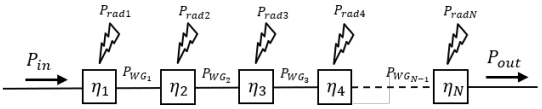

Fig. 7 Theoretical model of a grating antenna

The mathematical expressions are:

$$P_{in} = \sum_{i=1}^{N} P_{rad_i} + P_{out} \qquad (1)$$

$$P_{rad_j} = P_{in}\,\eta_j \prod_{i=1}^{j}(1-\eta_i) \qquad (2)$$

$$\eta_i = \frac{P_{rad_i}}{P_{WG_{i-1}}} \qquad (3)$$

where $P_{in}, P_{out}, P_{rad_i}$ and P_{WG_i} are the entrance, output, radiated in element *i* and propagated in element *i* powers, respectively. And η_i is the efficiency of radiation for a *i* radiation element. With these formulas and using a recursive method (Fig. 8), we can derive the internal antenna efficiency given a wanted radiating profile.

```
Eff_in(1) = Prad(1)/Pin;
PWG(1) = Pin - Prad(1);
for i = 2:length(x)
   Eff_in(i) = Prad(i)/PWG(i-1);
   PWG(i) = PWG(i-1) - Prad(i);
end
```

Fig. 8 Pseudo-code for calculation of η_i.

The next step in this study involves an investigation of the relation between the efficiency of antenna elements and their respective widths. To establish such a connection, a simulation approach has been employed, utilizing the simple model as the basis for analysis. If we considered a uniform antenna grating, it is clear that the antenna efficiencies will be the same, therefore the equation 2 will be:

$$P_{rad_j} = P_{in}\,\eta\,(1-\eta)^j \qquad (4)$$

And substituting in Eq. (1):

$$\frac{P_{in}-P_{out}}{P_{in}} = \eta\sum_{i=0}^{N}(1-\eta)^i \qquad (5)$$

As $(1-\eta) < 1$, we know that this series converges:

$$\sum_{i=0}^{N}(1-\eta)^i = \frac{1-(1-\eta)^{N+1}}{\eta} \qquad (6)$$

Therefore, we obtain a simple expression for the Normalized Power Radiated, defined as:

$$NPR = \frac{P_{in}-P_{out}}{P_{in}};\ NPR = 1-(1-\eta)^{N+1} \qquad (7)$$

Now, the relation between NPR and width, it is done using an electromagnetic simulation software (Lumerical FDTD). We have created a structure with a 50% duty cycle and $\Lambda = 0.66$ µm. In Fig. 9 are the results of doing a sweep varying the widths of every element of a 90-element uniform grating antenna from 0.5 μm (width of the original waveguide) up to 1 µm and we have recorded the NPR.

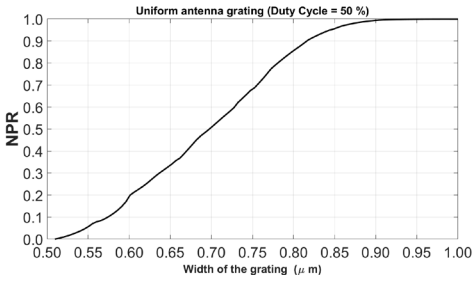

Fig. 9 Width sweep of a 90-element grating antenna

Combining data from Eq. (7) and from Fig. 9 we can derive a general relation between widths and efficiency of radiation for 50% duty cycle grating antenna.

5.2.- Results

For a 60-element grating antenna, using the method derived in section 5.1, we obtained the widths for each antenna element (Fig. 10) in order to obtain the ideal gaussian profile shown in Fig. 6.

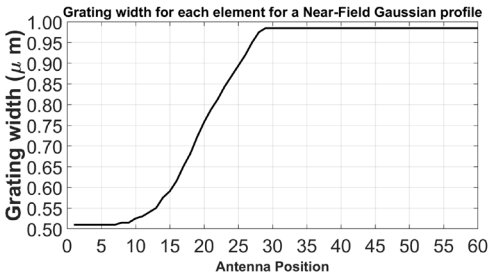

Fig. 10: Calculated grating width for i element.

After simulating the antenna structure considering the width changed along the length, and after a MATLAB post-processing, we derive the emitting near field profile compared with the wanted gaussian profile as it can be seen in Fig. 11.

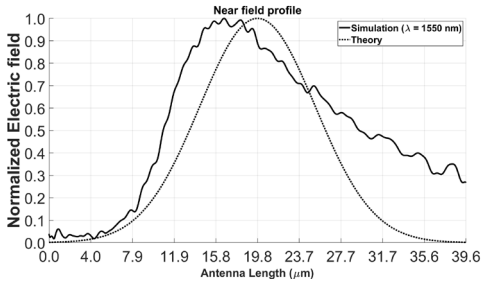

Fig. 11 Simulated near field profile in relation with the wanted profile.

Knowing the near fields, we can calculate the radiation pattern emitted by the antenna doing the spatial TF of the near field profile. In Fig. 12 is shown a comparison between the uniform grating antenna, the apodized grating antenna and the theoretical of a gaussian profile.

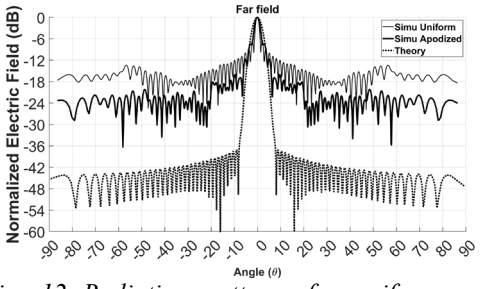

Fig. 12 Radiation patterns for uniform and apodized simulated antenna and ideal gaussian.

As illustrated in the results, a reduction in side lobe levels of 6-8 dB was achieved in all angles, except for the beam direction. As expected, we have seen a broadening in the beamwidth, being 1.3º for a uniform grating

antenna, 2º for an apodized antenna and 3º for a theoretical Gaussian. These widening can be compensated by elongating the antenna aperture size, increasing the number of antenna elements or via using the novel ultra-long grating antennas 0, which can theoretically present a beamwidth as small as 0.008º with a 10 mm antenna length.

6.- Conclusion

In this study, we proposed an approach for determining the optimal widths of grating antenna elements to achieve an arbitrary radiating profile in the context of INPERCEPT project. Future research directions could consider the effect of manufacturing resolution on the simulation results, explore alternative profile shapes, improving the theoretical model, and investigate the potential benefits of utilizing ultra-long gratings. Furthermore, our current approach focused solely on profile tailoring, without considering the impact of the propagating constant along the grating antenna, which governs the angle of emission. To further enhance the performance of the antenna, we intend to investigate the effect of duty cycle on phase change, in addition to modifying the grating widths for profile shaping.

References

[1] SAE J3016, "*Taxonomy and Definitions for Terms Related to Driving Automation Systems for On-Road Motor Vehicles"* J3016_202104, 2021

[2] "Mercedes-Benz world's first automotive company to certify SAE Level 3 system for U.S. market," *MBUSA Newsroom*, Jan. 2023

[3] Yeong, D.J. et al.,*"Sensor and Sensor Fusion Technology in Autonomous Vehicles: A Review"*. Sensors 2021

[4] W. Stark, et al,*"DCM Radar for Automotive Application,"* Uhnder White Paper, Jan. 2020

[5] T. M. Schmidl and D. Cox, *"Robust frequency and timing synchronisation for OFDM,"* IEEE Transactions on Communications, vol. 45, pp. 1613-1621, 1997

[6] D. Lahat, et al, *"Multimodal Data Fusion: An Overview of Methods, Challenges, and Prospects,"* Proc. IEEE 103(9), 2015, doi: 10.1109/JPROC.2015.2460697

[7] S. Chen, et al, *"3D Point Cloud Processing and Learning for Autonomous Driving: Impacting Map Creation, Localization, and Perception,"* in IEEE Sig. Proc. Mag, 38(1), 2021, doi: 10.1109/MSP.2020.2984780

[8] Luminar (NASDAQ: LAZR), Luminar. luminartech.com

[9] R. Nabati et al., *"CenterFusion: Center- Based Radar and Camera Fusion for 3D Object Detection,"* Proc. WACV 2021, doi: 10.1109/WACV48630.2021.00157

[10] Y. Long, et al, *"Radar-Camera Pixel Depth Association for Depth Completion,"* CVPR 2021, doi: 10.1109/CVPR46437.2021.01232

[11] BIS Research, Emerging Technology Market Intelligence, *"Global Automotive Lidar Market – Analysis and Forecast, 2018-2028"*, 2019

[12] Research and Markets, *"LIDAR technologies for the Automotive Industry: Technology benchmark, Challenges, Market forecasts"*, 2019

[13] Strategy Analytics, "Accelerating the Future: The Economic Impact of the Emerging Passenger Economy", Intel 2017

[14] M. E. Warren, *"Automotive LIDAR Technology,"* 2019 Symposium on VLSI Circuits, Kyoto, Japan, 2019, pp. C254-C255, doi: 10.23919/VLSIC.2019.8777993

[15] F. C. Delori, et al., *"Maximum permissible exposures for ocular safety (ANSI 2000), with emphasis on ophthalmic devices,"* J. Opt. Soc. Am. A, 24(5), pp. 1250–1265, 2007

[16] A.E.Limet al., *"Review of silicon photonics foundry efforts,"*, IEEE J. Sel. Topics Quantum Electron., 20(4), pp. 405–416, Jul./Aug. 2013

[17] R. Baets et al., *"Silicon photonics: Silicon nitride versus silicon-on-insulator,"* 2016 Optical Fiber Communications Conference and Exhibition (OFC), Anaheim, CA, USA, 2016, pp. 1-3.

[18] C. -P. Hsu et al., *"A Review and Perspective on Optical Phased Array for Automotive LiDAR,"* in IEEE Journal of Selected Topics in Quantum Electronics, 27(1) 2021, Art no. 8300416, doi: 10.1109/JSTQE.2020.3022948

[19] C. V. Poulton et al., *"Large-scale silicon nitride nanophotonic phased arrays at infrared and visible wavelengths,"* Opt. Lett., 42(1), pp. 21–24, Jan. 2017

[20] A. A. Oliner, *"Leaky-wave antennas,"* in Antenna Engineering Handbook, 3rd ed., R. C. Johnson, Ed. Georgia: McGraw-Hill, 1993, ch. 10

[21] Lei Yu, et al. *"Adoption of large aperture chirped grating antennas in optical phase array for long distance ranging,"* Opt. Express 30, 28112-28120 (2022)

Nie, X., *"Design of ultra-long waveguide grating antennas with uniform emission and high directionality for optical phased arrays on a silicon-on-insulator waveguide platform"*, Optics Communications 531, 2023. doi:10.1016/j.optcom.2022.129210